

Three-dimensional antiferromagnetic CP^{N-1} models

Francesco Delfino,¹ Andrea Pelissetto,² and Ettore Vicari¹

¹*Dipartimento di Fisica dell'Università di Pisa and INFN, Largo Pontecorvo 3, I-56127 Pisa, Italy*

²*Dipartimento di Fisica dell'Università di Roma "La Sapienza" and INFN, Sezione di Roma I, I-00185 Roma, Italy*

(Received 3 March 2015; published 8 May 2015)

We investigate the critical behavior of three-dimensional antiferromagnetic CP^{N-1} (ACP^{N-1}) models in cubic lattices, which are characterized by a global $U(N)$ symmetry and a local $U(1)$ gauge symmetry. Assuming that critical fluctuations are associated with a staggered gauge-invariant (Hermitian traceless matrix) order parameter, we determine the corresponding Landau-Ginzburg-Wilson (LGW) model. For $N = 3$ this mapping allows us to conclude that the three-component ACP^2 model undergoes a continuous transition that belongs to the $O(8)$ vector universality class, with an effective enlargement of the symmetry at the critical point. This prediction is confirmed by numerical analyses of the finite-size scaling behaviors of the ACP^2 and the $O(8)$ vector models, which show the same universal features at their transitions. We also present a renormalization-group (RG) analysis of the LGW theories for $N \geq 4$. We compute perturbative series in two different renormalization schemes and analyze the corresponding RG flow. We do not find stable fixed points that can be associated with continuous transitions.

DOI: [10.1103/PhysRevE.91.052109](https://doi.org/10.1103/PhysRevE.91.052109)

PACS number(s): 05.70.Jk, 05.10.Cc, 05.70.Fh

I. INTRODUCTION

CP^{N-1} models are a class of models in which the fundamental field is a complex N -component unit vector (more precisely, an element of the complex projective manifold CP^{N-1}), and which are characterized by a global $U(N)$ symmetry and a local $U(1)$ gauge symmetry. They emerge as effective theories of $SU(N)$ quantum antiferromagnets [1–4] and of scalar electrodynamics with a compact $U(1)$ gauge group. The simplest three-dimensional (3D) CP^{N-1} lattice model is defined by the Hamiltonian

$$H = J \sum_{\langle ij \rangle} |\bar{z}_i \cdot z_j|^2, \quad (1)$$

where the sum is over the nearest-neighbor sites of a cubic lattice, z_i are N -component complex vectors satisfying $\bar{z}_i \cdot z_i = 1$. The model is ferromagnetic for $J < 0$, antiferromagnetic for $J > 0$.

The CP^1 model can be mapped onto the $O(3)$ -symmetric Heisenberg model. Indeed, if one defines $O(3)$ spins $s_i^\alpha = \sum_{ab} \bar{z}_i^a \sigma_{ab}^\alpha z_i^b$, where σ^α are the Pauli matrices, one can rewrite the CP^1 Hamiltonian as that of the usual 3-vector Heisenberg model. As a consequence, the critical properties can be straightforwardly derived by using the wealth of results available for the Heisenberg model (see, e.g., Refs. [5–7]). On the other hand, several aspects of the phase behavior of CP^{N-1} models with $N > 2$ remain unclear and worth being further investigated.

The critical behavior of CP^{N-1} models can be investigated by constructing an effective Landau-Ginzburg-Wilson (LGW) theory. This approach requires the identification of the order parameter associated with the critical modes. A plausible choice for ferromagnetic ($J < 0$) systems is the gauge-invariant site variable [2,8]

$$Q_i^{ab} = \bar{z}_i^a z_i^b - \frac{1}{N} \delta^{ab}, \quad (2)$$

which is a Hermitian and traceless $N \times N$ matrix. In the corresponding LGW theory, the fundamental field is therefore the most general traceless Hermitian matrix $\Phi^{ab}(x)$, which

one can imagine being defined as the average of Q_i^{ab} over a large but finite lattice domain. The Hamiltonian is the most general fourth-order polynomial in Φ consistent with the $U(N)$ symmetry:

$$\mathcal{H} = \text{Tr}(\partial_\mu \Phi)^2 + r \text{Tr} \Phi^2 + w \text{tr} \Phi^3 + u (\text{Tr} \Phi^2)^2 + v \text{Tr} \Phi^4. \quad (3)$$

For $N = 2$, one recovers the $O(3)$ -symmetric LGW theory because the cubic term vanishes and the two quartic terms are equivalent [9], consistently with the equivalence between the CP^1 and the Heisenberg model. Because of the presence of the cubic term, on the basis of mean-field arguments, one expects the system to undergo a first-order transition for any $N > 2$, unless the Hamiltonian parameters are tuned so that $w = 0$ in the effective model. This prediction is, however, contradicted by recent numerical studies [2,8,10,11], which find evidence of continuous transitions in models that are expected to be in the same universality class as that of the 3D CP^2 model. In particular, a numerical study of 3D loop models [8] provided the estimate $\nu = 0.536(13)$ for the correlation-length critical exponent. These results imply the existence of a 3D CP^2 universality class characterized by a $U(3)$ global symmetry and $U(1)$ gauge invariance, with a corresponding fixed point (FP) that cannot be determined in perturbation theory at fixed N . In order to access this FP, the authors of Ref. [8] proposed a double expansion around $N = 2$ (where the cubic term vanishes) and $\epsilon = 4 - d$, arguing that a continuous transition may be possible for values of N sufficiently close to $N = 2$. For larger values of N , i.e., $N \geq 4$, the numerical analyses [2,8,10] show evidence of first-order transitions. In the large- N limit, the quantum field theory corresponding to the ferromagnetic CP^{N-1} model gives rise to an effective Abelian Higgs model and Landau-Ginzburg (LG) theory of superconductivity [12], whose renormalization-group (RG) flow presents a stable FP for a sufficiently large number of components. Thus, continuous transitions are again possible in CP^{N-1} models at large N , sharing the same universal critical behaviors of the LG theory of superconductivity [12]. These results are again in contrast with the conclusions obtained from the LGW theory

(3) and suggest that, at least for large values of N , critical modes are not exclusively associated with the gauge-invariant order parameter Q [cf. Eq. (2)], but other features become relevant.

In this paper, we investigate the critical behavior of antiferromagnetic CP^{N-1} (ACP^{N-1}) models, such as those described by the Hamiltonian (1) with $J > 0$, on a cubic lattice (we expect a similar behavior on any bipartite lattice). For $N = 2$, they undergo a critical transition in the same universality class as that of the ferromagnetic CP^1 model. Indeed, the ACP^1 model is equivalent to the antiferromagnetic Heisenberg model, which in turn can be mapped onto the ferromagnetic one by performing the transformation $s(x) \rightarrow (-1)^{x_1+x_2+x_3}s(x)$, where $x \equiv (x_1, x_2, x_3)$. Therefore, the staggered variables $s_{\text{stag}} = (-1)^{x_1+x_2+x_3}s$ or $Q_{\text{stag}} = (-1)^{x_1+x_2+x_3}Q$ have the same critical behavior as s or Q in the ferromagnetic model. However, for $N > 2$ the behavior of ACP^{N-1} models differs from that of ferromagnetic CP^{N-1} models, as we shall show.

Under the assumption that the critical modes can be represented by staggered local gauge-invariant variables, we show that the LGW Hamiltonian describing the behavior of the critical modes in the ACP^{N-1} models is the one given in Eq. (3), without the cubic term, that is with $w = 0$. Indeed, the staggered nature of the order parameter gives rise to a symmetry $\Phi \rightarrow -\Phi$, which prevents the presence of odd terms in Φ , such as the cubic term. This fact greatly simplifies the RG analysis of the theory. In particular, it allows us to predict that the critical behavior of the ACP^2 model belongs to the universality class of the $O(8)$ vector model, with a dynamical enlargement of the symmetry at the critical point. Correspondingly, we predict $\nu \approx 0.85$ for the ACP^2 model, which differ from that found in Refs. [8,10] for the ferromagnetic CP^2 universality class. To validate this prediction, we perform Monte Carlo (MC) simulations of the lattice ACP^2 and $O(8)$ vector models. The critical exponents and finite-size scaling (FSS) functions turn out to be the same in the two models, in agreement with the RG argument. Finally, we present a general RG study of the LGW theory (3) without cubic term. We compute high-order field-theoretical (FT) perturbative series in two different schemes. The RG analysis does not provide evidence of the existence of stable FPs for $N \geq 4$.

We mention that a critical-point symmetry enlargement analogous to that of ACP^2 models occurs in the antiferromagnetic RP^2 model [13,14]. These systems are similar to those considered here: their Hamiltonian is also given by Eq. (1), but the site variable is a *real* unit vector. Analogously to the case of the ACP^2 model, RG arguments based on the corresponding LGW theory predict that the critical behavior of the antiferromagnetic RP^2 model belongs to the universality class of the $O(5)$ vector model.

The paper is organized as follows. In Sec. II, we construct the LGW theory which is expected to describe the critical modes at continuous transitions of ACP^{N-1} models, assuming a staggered gauge-invariant order parameter. Section III is devoted to a numerical study of the ACP^2 model. We show that its continuous transition is in the same universality class as that of the $O(8)$ vector model. In Sec. IV, we study the RG flow relevant for models with more components, i.e., for

$N \geq 4$, computing and analyzing high-order FT perturbative series for the corresponding LGW theories. Finally, in Sec. V we summarize our main results and draw some conclusions. Some details are reported in the Appendixes.

II. LGW THEORY FOR THE ACP^{N-1} MODELS

We now derive the LGW theory for the critical modes at the transition in ACP^{N-1} models. This effective theory is generally constructed using global properties such as the symmetry of the model, the nature of the order parameter, and the symmetry-breaking pattern. In the case at hand, the model has a global $U(N)$ symmetry and a local $U(1)$ gauge invariance. We assume that the critical modes are effectively represented by local gauge-invariant variables, such as (2). In the case of antiferromagnetic interactions ($J > 0$), the minimum of the Hamiltonian (1) is locally realized by taking $\bar{z}_i \cdot z_j = 0$ for any pair of nearest-neighbor sites.

In order to construct the LGW Hamiltonian, we should identify the order parameter of the transition. At variance with the ferromagnetic case, in the ACP^{N-1} model we should take into account the explicit breaking of translational invariance in the low-temperature phase. To clarify the issue, let us consider the antiferromagnetic $O(M)$ vector model with Hamiltonian $H_O = \sum_{\langle ij \rangle} s_i \cdot s_j$. In this case, the order parameter is $\phi = \sum_x p_x s_x$, where p_x is the parity of the site $x \equiv (x_1, x_2, x_3)$ defined by $p_x = (-1)^{\sum_i x_i}$. Under translations of one site, we find $\phi \rightarrow -\phi$, hence, this parameter allows us to probe the breaking of translational invariance. In the ACP^{N-1} model, the natural field variable is the combination $\bar{z}_i^a z_i^b$, which is invariant under the local $U(1)$ gauge transformations of the model. Hence, we define the order parameter

$$B^{ab} = \sum_x p_x \bar{z}_x^a z_x^b. \quad (4)$$

It is immediate to verify that B is Hermitian and traceless (this follows from the presence of p_x), that it changes sign under translations of one site which exchange the two sublattices, and that it coincides with the $O(3)$ order parameter for $N = 2$. Then, as usual, in order to construct the LGW model, we replace B with a local variable Ψ as fundamental variable (essentially, one may imagine that Ψ is defined as B , but now the summation extends only over a large, but finite, cubic sublattice). Then, we write the most general fourth-order polynomial that is invariant under $U(N)$ transformations and under the \mathbb{Z}_2 transformation $\Psi \rightarrow -\Psi$, a consequence of the translation invariance of the original theory. We obtain

$$\mathcal{H}_a = \text{Tr}(\partial_\mu \Psi)^2 + r \text{Tr} \Psi^2 + \frac{u_0}{4} (\text{Tr} \Psi^2)^2 + \frac{v_0}{4} \text{Tr} \Psi^4. \quad (5)$$

The original $U(N)$ symmetry corresponds to the symmetry $\Psi \rightarrow U^\dagger \Psi U$ where $U \in U(N)$. The order parameter Ψ is a Hermitian traceless matrix as the variable Φ introduced in the ferromagnetic case. However, because of the presence of the symmetry $\Psi \rightarrow -\Psi$, which is a specific feature of the antiferromagnetic model, the LGW Hamiltonian (5) does not present a cubic term, which instead appears in the Φ^4 Hamiltonian (3) corresponding to the ferromagnetic case.

Note that the model is not only characterized by the symmetry group, but also by the nature of the order parameter.

There are indeed other models with U(*N*) symmetry (see, e.g., Ref. [15] for an example), which, however, have a different order parameter and different symmetry-breaking patterns, leading to different universality classes.

The stability domain of \mathcal{H}_a can be determined by studying the asymptotic behavior of the potential

$$V(\Psi) = r \text{Tr} \Psi^2 + \frac{u_0}{4} (\text{Tr} \Psi^2)^2 + \frac{v_0}{4} \text{Tr} \Psi^4. \quad (6)$$

This analysis can be easily performed by noting that $V(\Psi)$ only depends on the N real eigenvalues λ_a of the Hermitian matrix Ψ , which satisfy the condition $\sum_a \lambda_a = 0$. We find that the theory is stable if

$$u_0 + b_N v_0 > 0, \quad b_N = \frac{N^2 - 3N + 3}{N(N-1)}, \quad (7)$$

and if

$$\begin{aligned} u_0 + \frac{1}{N} v_0 > 0 & \quad \text{for even } N, \\ u_0 + c_N v_0 > 0 & \quad \text{for odd } N, \end{aligned} \quad (8)$$

where

$$c_N = \frac{N^2 + 3}{N(N^2 - 1)}. \quad (9)$$

Physical systems corresponding to the effective theory (5) with u_0, v_0 that do not satisfy these constraints are expected to undergo a first-order phase transition.

The analysis of the minima of the potential $V(\Psi)$ for $r < 0$ gives us information on the symmetry-breaking patterns. For $v_0 < 0$, the absolute minimum of $V(\Psi)$ is realized by configurations with $\Psi = U \Psi_{\min} U^\dagger$ and

$$\Psi_{\min} \sim \begin{pmatrix} I_{N-1} & 0 \\ 0 & -(N-1) \end{pmatrix}, \quad (10)$$

where I_n indicates the $n \times n$ identity matrix. This gives rise to the symmetry-breaking pattern

$$U(N) \rightarrow U(1) \times U(N-1). \quad (11)$$

On the other hand, for $v_0 > 0$ and even N the minimum is realized by

$$\Psi_{\min} \sim \begin{pmatrix} I_{N/2} & 0 \\ 0 & -I_{N/2} \end{pmatrix} \quad (12)$$

implying the symmetry-breaking pattern

$$U(N) \rightarrow U(N/2) \times U(N/2). \quad (13)$$

For $v_0 > 0$ and odd values of N , we have instead

$$\Psi_{\min} \sim \begin{pmatrix} I_{(N+1)/2} & 0 \\ 0 & -k I_{(N-1)/2} \end{pmatrix}, \quad (14)$$

$k = (N+1)/(N-1)$, so that

$$U(N) \rightarrow U(N/2 + 1/2) \times U(N/2 - 1/2). \quad (15)$$

Note that for $N = 3$, the symmetry-breaking patterns (11) and (15) are equivalent, hence, the sign of v_0 does not play any role.

An important remark is in order. The derivation of the LGW Hamiltonian (5) is based on the assumption that the

order parameter is the staggered and traceless Hermitian matrix (4). This assumption can be checked for $N = 3$. As we show in Appendix A, the minimum-energy configurations of Hamiltonian (1) for $J > 0$ have a very simple structure. Modulo a global U(3) transformation, one can take $\mathbf{z}_i = (1, 0, 0)$ on one sublattice, and $\mathbf{z}_i = (0, a_i, b_i)$ on the other one. Hence, a zero-temperature configuration corresponds to

$$B \sim \begin{pmatrix} 1 & 0 & 0 \\ 0 & -\sum_i |a_i|^2 & -\sum_i a_i^* b_i \\ 0 & -\sum_i a_i b_i^* & -\sum_i |b_i|^2 \end{pmatrix}. \quad (16)$$

Therefore, B is nonvanishing in the low-temperature phase and represents the correct order parameter. The symmetry-breaking pattern is that given in Eq. (11) or, equivalently, Eq. (15).

For $N \geq 4$, we have not been able to identify ordered zero-temperature configurations that are translation invariant at least on one sublattice, hence, we have not been able to check that B , as defined in Eq. (4), is nonvanishing in the low-temperature phase, hence that it can be taken as the order parameter. In the following, we make the working hypothesis that this is the case, determining what this assumption implies for the nature of the transitions in the ACP^{N-1} models.

For $N = 3$, the LGW theory (5) simplifies. Indeed, one can easily prove that

$$\text{Tr} \Psi^4 = \frac{1}{2} (\text{Tr} \Psi^2)^2 \quad (17)$$

for any 3×3 traceless Hermitian matrix. Then, let us define an eight-component real vector field ϕ as follows:

$$\begin{aligned} \frac{\Psi_{11} + a_+ \Psi_{22}}{\sqrt{2}} &= \phi_1, & \frac{\Psi_{11} + a_- \Psi_{22}}{\sqrt{2}} &= \phi_2, \\ \Psi_{12} &= \phi_3 + i\phi_4, & \Psi_{13} &= \phi_5 + i\phi_6, & \Psi_{23} &= \phi_7 + i\phi_8, \end{aligned} \quad (18)$$

where $a_{\pm} = (1 \pm \sqrt{3})/2$. In terms of the field ϕ we have

$$\frac{1}{2} \text{Tr} \Psi^2 = \phi \phi. \quad (19)$$

Then, we can rewrite \mathcal{H}_a as

$$\mathcal{H}_O = (\partial_\mu \phi)^2 + 2r \phi^2 + g_0 (\phi^2)^2, \quad (20)$$

where $g_0 \equiv u_0 + v_0/2$, proving that the model is equivalent to the O(8) vector theory.

Since the O(8) vector theory has a stable Wilson-Fisher FP, the above correspondence allows us to predict that the critical behavior of the ACP² model must share the same universal features as the 3D O(8) vector model. Note that the enlargement of the symmetry to O(8) is a feature of the LGW theory (5), i.e., of the expansion up to fourth powers of Ψ . Indeed, one can easily check that the sixth-order terms allowed by the U(3) symmetry, such as $\text{Tr} \Psi^6$, do not share the O(8) symmetry. Since these terms are RG irrelevant at the O(8) FP, the contribution of the terms breaking the O(8) symmetry is suppressed at the critical point. In this sense, we have a dynamic enlargement of the symmetry to O(8) at the critical point.

Of course, the fact that only one quartic term is independent for $N = 3$ holds also for the Hamiltonian (3) corresponding to the ferromagnetic CP² model. Thus, it has an O(8) FP, which is

unstable due to the presence of the cubic term. This cubic term gives rise to a spin-3 perturbation at the O(8) FP [16], i.e., a RG perturbation belonging to the spin-3 representation of the O(8) group. Its RG dimension y_3 can be estimated using the results of Ref. [17] for the crossover exponent ϕ_3 , i.e., $y_3 = \phi_3/\nu$. The crossover exponent ϕ_3 at the O(8) FP was estimated in Ref. [17], obtaining $\phi_3 = 0.97(3)$ in the fixed-dimension massive-zero-momentum scheme, and $\phi_3 = 0.95(5)$ in the ϵ expansion. Since $\nu = 0.85(2)$ (see Sec. III B), we obtain $y_3 \approx 1.1$. As $y_3 > 0$, the O(8) FP is unstable in the presence of the cubic term, and, therefore, the O(8) FP cannot be the stable FP in the case of ferromagnetic interactions. This is confirmed by the results of Refs. [8,10]. The critical exponents, for instance $\nu = 0.536(13)$, significantly differ from those of the O(8) universality class.

It is worth mentioning that an analogous enlargement of the symmetry at the critical point is also observed [13,14] in the antiferromagnetic RP^2 model. The Hamiltonian of RP^{N-1} models is analogous to that of CP^{N-1} models. It is given by Eq. (1), with real N -component spins s_i replacing the complex vectors z_i . The order parameter should be a symmetric and traceless $N \times N$ matrix Σ , analogous to the matrix B defined in Eq. (4). The corresponding LGW Hamiltonian is given in Eq. (5), with Ψ replaced by Σ [13,14]. For $N = 3$, the two quartic terms are proportional, and one obtains the Φ^4 theory of the O(5) vector model [again high-order terms break the O(5) symmetry, but since they are irrelevant, the O(5) symmetry breaking is suppressed in the critical limit]. The numerical results of Refs. [13,14] for the antiferromagnetic RP^2 model confirm this prediction.

To identify the nature of a critical transition for $N \geq 4$, if it exists, we must determine the FPs of the RG flow of the LGW theory (5). The absence of a stable FP implies the absence of continuous transitions. Such an analysis is quite complex, due to the presence of two quartic terms. We will perform it in Sec. IV.

III. CRITICAL BEHAVIOR OF THE ACP² LATTICE MODEL

We now check the predictions of the previous section for the critical behavior of the 3D ACP² model, confirming that it undergoes a continuous transition in the O(8) universality class.

A. Monte Carlo simulations and observables

In order to study the critical behavior of the ACP² lattice model (1) with $J = 1$, we perform Monte Carlo simulations of cubic systems of linear size L with periodic boundary conditions. Because of the antiferromagnetic nature of the model we take L even. We use a standard Metropolis algorithm, hence, we are only able to obtain reliable results up to $L = 40$. We use a simple updating algorithm. If $\varphi = (\text{Re } z, \text{Im } z)$ is a six-component vector, the update consists in proposing the new vector $R\varphi$, where R is a random O(2) matrix acting on two randomly chosen components of φ .

In our MC simulations, we compute correlations of the gauge-invariant operator

$$P_x^{ab} = \bar{z}_x^a z_x^b. \quad (21)$$

Its two-point correlation function is defined as

$$G(x - y) = \langle \text{Tr } P_x^\dagger P_y \rangle = \langle |\bar{z}_x \cdot z_y|^2 \rangle. \quad (22)$$

Due to the staggered nature of the ordered parameter, we should distinguish correlations between points belonging to the same sublattice and points belonging to different sublattices. Here, we define the susceptibility and the correlation length by summing only over points with the same parity:

$$\chi = \sum_{x \text{ even}} G(x) = \tilde{G}(0), \quad (23)$$

$$\xi^2 \equiv \frac{1}{4 \sin^2(p_{\min}/2)} \frac{\tilde{G}(0) - \tilde{G}(p)}{\tilde{G}(p)}, \quad (24)$$

where x runs over all even points,

$$\tilde{G}(p) = \sum_{x \text{ even}} e^{ip \cdot x} G(x) \quad (25)$$

is the Fourier transform of $G(x)$ over the even sublattice, $p = (p_{\min}, 0, 0)$, and $p_{\min} \equiv 2\pi/L$. Finally, we consider the Binder parameter

$$U = \frac{\langle [\sum_{x \text{ even}} \text{Tr } P_0^\dagger P_x]^2 \rangle}{\langle \sum_{x \text{ even}} \text{Tr } P_0^\dagger P_x \rangle^2}. \quad (26)$$

In the FSS limit, any RG invariant quantity R , such as $R_\xi \equiv \xi/L$ and U , is expected to behave as

$$R(\beta, L) = f_R(X) + L^{-\omega} g_R(X) + \dots, \quad (27)$$

where $X = (\beta - \beta_c)L^{1/\nu}$ and $f_R(X)$ is a universal function apart from a trivial normalization of the argument. In particular, the quantity $R^* \equiv f_R(0)$ is universal within the given universality class. The approach to the asymptotic behavior is controlled by the universal exponent $\omega > 0$, which is associated with the leading irrelevant RG operator. Around β_c one may expand $f_R(X)$ and $g_R(X)$ in powers of the scaling variable X , obtaining

$$R = R^* + \sum_{n=1} b_n (\beta - \beta_c)^n L^{n/\nu} + L^{-\omega} \sum_{n=0} c_n (\beta - \beta_c)^n L^{n/\nu} + \dots \quad (28)$$

The exponent η is determined by analyzing the FSS behavior of the susceptibility

$$\chi \sim L^{2-\eta} [f_\chi(X) + O(L^{-\omega})]. \quad (29)$$

We present a FSS analysis of the numerical data of the ACP² lattice model, up to $L = 40$. In Fig. 1, we show MC data of $R_\xi \equiv \xi/L$ for several values of L . They show a crossing point, providing evidence of a transition in the interval $4.1 \lesssim \beta \lesssim 4.2$. An analogous behavior is shown by the Binder parameter U .

To determine whether the transition is continuous or of first order, we should estimate the effective exponent ν that gives the slope of the data at the critical point. At a first-order transition we expect $\nu = 1/d = 1/3$ [18–20], while $\nu > 1/d$ at continuous transitions. The numerical data, including those of the specific heat, definitely exclude a first-order transition. Indeed, the increase of $dR/d\beta$ at the crossing point is much

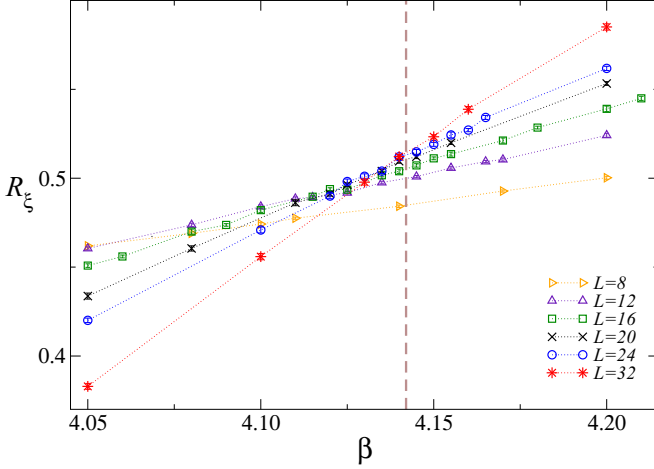


FIG. 1. (Color online) MC data of R_ξ for the ACP^2 lattice model for several lattice sizes L . They show a crossing point at $\beta \approx 4.14$. The dotted lines are drawn to guide the eye. The dashed vertical line corresponds to our best estimate (34) of β_c obtained by a FSS analysis of the available data assuming the transition to belong to the $O(8)$ universality class.

slower than L^3 . Therefore, we conclude that the ACP^2 model has a continuous transition.

B. 3D $O(8)$ vector model

To show that the ACP^2 lattice model belongs to the $O(8)$ universality class, we show that critical exponents and FSS curves are the same in the two models. Thus, we begin by computing these quantities in the $O(8)$ spin model defined by the Hamiltonian

$$H_O = - \sum_{\langle ij \rangle} \mathbf{s}_i \cdot \mathbf{s}_j, \quad (30)$$

where the spin variable \mathbf{s}_i is an eight-component unit vector. We consider cubic systems of linear size L with periodic boundary conditions.

We consider the two-point function

$$G_o(x-y) = \langle \mathbf{s}_x \cdot \mathbf{s}_y \rangle, \quad (31)$$

and compute the corresponding susceptibility and second-moment correlation length. They are defined as in Eqs. (23) and (24), but now we sum over all lattice points, as the model is ferromagnetic. Moreover, we consider the Binder parameter U defined as in Eq. (26): we replace P_x with s_x and sum over all lattice points.

We perform simulations on lattices of size up to $L = 96$ (we use a cluster algorithm) and estimate R_ξ , U , and χ . To compute the critical exponents we fit the data to Eqs. (27) and (29). In the analysis, we take into account the scaling corrections of order $L^{-\omega}$, fixing $\omega \approx 0.8$, as predicted by the FT perturbative analyses discussed in the following. Corrections turn out to be small, hence the analyses of the MC data are unable to provide a more accurate estimate of ω . Fits of R_ξ to Eq. (28) (we take the first terms in the expansions) give $\beta_c = 1.92677(2)$,

$$\nu = 0.85(2), \quad \eta = 0.0276(5), \quad (32)$$

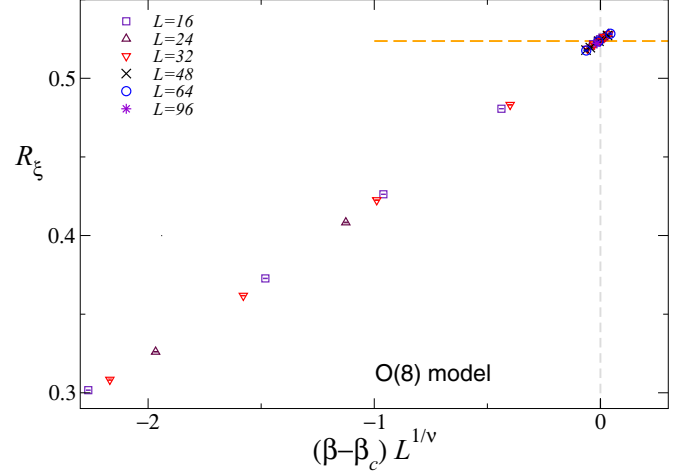


FIG. 2. (Color online) FSS behavior of the MC data of R_ξ for the $O(8)$ vector model. Plot of R_ξ versus $(\beta - \beta_c)L^{1/\nu}$, setting $\beta_c = 1.92677$ and $\nu = 0.85$. The dashed horizontal line corresponds to $R_\xi = 0.5237$.

and the universal critical value $R_\xi^* = 0.5237(4)$. The quoted uncertainty includes the statistical error and the variation of the estimates as ω varies between 0.75 and 0.85, an interval that is larger than that obtained in the FT analyses reported below. In Fig. 2, we show R_ξ versus $(\beta - \beta_c)L^{1/\nu}$ using the above-reported estimates. Data collapse onto a single curve, confirming the accuracy of the estimates. Consistent results are obtained from the analysis of the Binder parameter, which also gives $U^* = 1.0383(3)$.

The values of the critical exponents can be compared with previous results. Field theory gives $\nu \approx 0.830$ and $\eta \approx 0.027$ [21], while the analysis of strong-coupling expansions gives $\nu \approx 0.84, 0.86$ [22] (the two estimates are obtained by means of two different resummation methods). Within errors, they agree with the estimates (32). We have repeated the analysis of the available six-loop series within the massive zero-momentum renormalization scheme [21,23], using the conformal mapping method that exploits the known large-order behavior of the perturbative expansions [24,25]. We obtain $\nu = 0.826(4)$, $\eta = 0.025(1)$, and $\omega = 0.81(1)$, where the errors are related to the change of the estimates with respect to a (reasonable) variation of the parameters entering the resummation procedure. They are substantially consistent with our favorite MC estimates (32), although one may suspect that errors are slightly underestimated. The FT analysis also provides the estimate of ω that we used (note that, to be on the safe side, we allowed for a much larger uncertainty in the MC analysis).

C. FSS of the ACP^2 lattice model

If the transitions in the ACP^2 and $O(8)$ models belong to the same universality class, critical exponents and FSS curves $f_R(X)$ for RG invariant quantities (apart from a trivial rescaling of the variable X) should be the same. This is what we check in the following.

A first unbiased universality check, which does not need an estimate of the critical point β_c , is obtained by plotting R_ξ

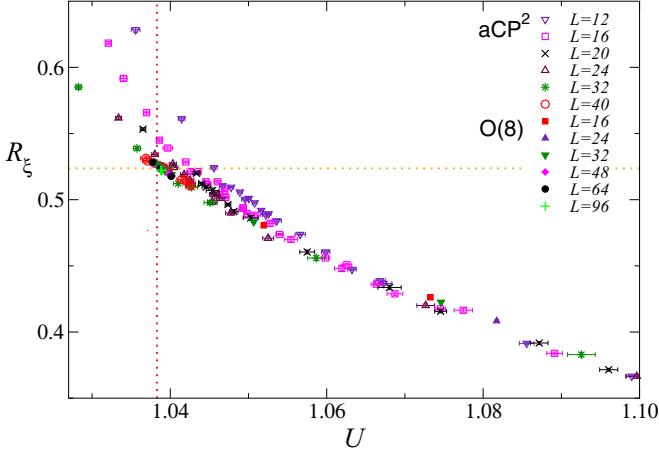


FIG. 3. (Color online) Plot of R_ξ vs U . The ACP² and O(8) MC results approach the same asymptotic curve. The dotted horizontal and vertical lines correspond to the critical values $R_\xi^* \approx 0.5237$ and $U^* \approx 1.0383$ estimated in the O(8) vector model.

versus U . Indeed, since both R_ξ and U satisfy Eq. (27), we must have

$$R_\xi = F(U) + O(L^{-\omega}), \quad (33)$$

where $F(U)$ is a universal function. In Fig. 3, we compare the results for the two models: they appear to approach the same asymptotic curve with increasing the lattice size. Scaling corrections are consistent with the expected $L^{-\omega}$ behavior with $\omega \approx 0.8$. They are much smaller for $\beta < \beta_c$ than for $\beta > \beta_c$.

The dependence of the data on the inverse temperature β around the crossing point is consistent with the O(8) results. Fits of the data around the crossing point to the first few terms of the expansions appearing in Eq. (28) provide an accurate estimate of the critical point,

$$\beta_c = 4.142(1). \quad (34)$$

In Fig. 4, we show $\chi L^{\eta-2}$ and R_ξ versus X , using the estimate (34) of β_c and the O(8) estimates (32) of the critical exponents. The data approach asymptotic scaling curves. Scaling corrections are larger for R_ξ , but definitely compatible with the expected $L^{-\omega}$ behavior. Note also (not shown) that the scaling curves of R_ξ for the ACP² and O(8) nicely match after a trivial rescaling of the scaling variable $(\beta - \beta_c)L^{1/\nu}$: if we define $Y = X$ for the ACP² and $Y = 3.9X$ for the O(8) model, all data fall on the same curve when plotted versus Y . Finally, we consider the specific heat C_v at β_c . We expect $C_v \approx a + cL^{\alpha/\nu}$ with $\alpha/\nu = 2/\nu - 3 \approx -0.67$. The MC data are consistent with this behavior.

In conclusion, the numerical analysis of the ACP² lattice model provides a robust evidence that its continuous transition belongs to the universality class of the O(8) vector model, as predicted by the RG arguments of Sec. II.

IV. RG FLOW FOR $N \geq 4$

In this section, we present a FT study of the RG flow of the LGW theory (5) with $N \geq 4$, i.e., the most general Φ^4 theory with traceless Hermitian $N \times N$ matrix fields and parity symmetry. The critical behavior at a continuous transition is

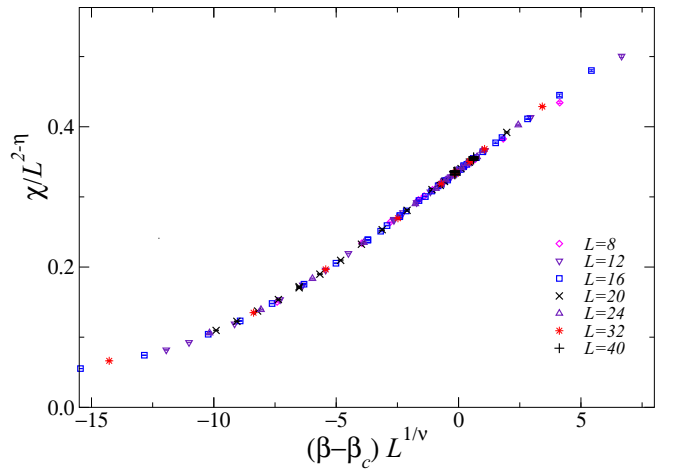
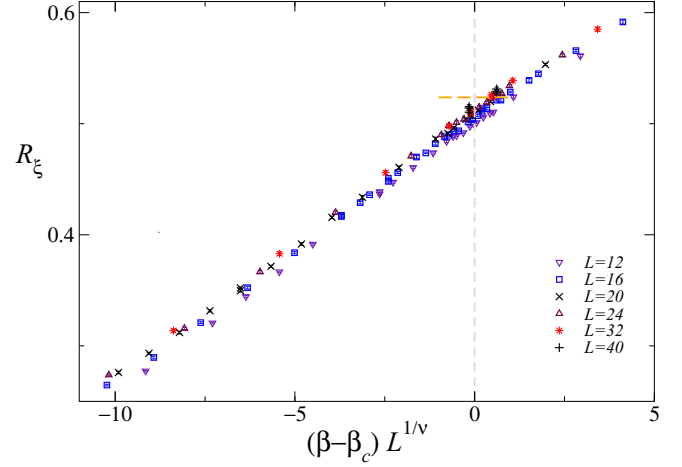


FIG. 4. (Color online) Scaling behavior of the ratios $\chi/L^{2-\eta}$ and R_ξ vs $(\beta - \beta_c)L^{1/\nu}$ with $\beta_c = 4.142$ and the critical exponents of the O(8) universality class [cf. Eq. (32)]. In the top figure, the dashed horizontal segment indicates the O(8) universal value $R_\xi = 0.5237$, which is clearly approached by the data of the ACP² lattice model with increasing L .

controlled by the FPs of the RG flow, which are determined by the common zeros of the β functions associated with the quartic parameters. The presence of a stable FP controls the universal features of the critical behavior in the case of continuous transition. The absence of a stable FP implies the absence of a corresponding universality class, hence a transition characterized by the same symmetry-breaking pattern must be of first order.

A. $\overline{\text{MS}}$ perturbative scheme

We compute the β functions of the quartic couplings in the $\overline{\text{MS}}$ renormalization scheme [26], which uses the dimensional regularization around four dimensions, and the modified minimal-subtraction prescription. Thus, the RG functions are obtained from the divergences for $\epsilon \equiv 4 - d \rightarrow 0$ appearing in the perturbative expansion of the correlation functions of the critical massless theory.

The procedure is straightforward (see, e.g., Ref. [27]). The renormalized couplings are defined from the irreducible

four-point correlation function, and the $\overline{\text{MS}}$ β functions are

$$\beta_u(u, v) = \mu \frac{\partial u}{\partial \mu} \Big|_{u_0, v_0}, \quad \beta_v(u, v) = \mu \frac{\partial v}{\partial \mu} \Big|_{u_0, v_0}, \quad (35)$$

where μ is the renormalization energy scale of the $\overline{\text{MS}}$ scheme. Here, u and v are the renormalized couplings corresponding to u_0 , v_0 , defined so that $u \propto u_0/\mu^\epsilon$ and $v \propto v_0/\mu^\epsilon$ at the lowest order. We compute the β functions up to five loops. The complete series for $N = 4$ are reported in Appendix B.

1. One-loop analysis close to four dimensions

Let us first analyze the one-loop β functions. They read as

$$\beta_u = -\epsilon u + \frac{N^2 + 7}{6} u^2 + \frac{2N^2 - 3}{3N} uv + \frac{N^2 + 3}{2N^2} v^2, \quad (36)$$

$$\beta_v = -\epsilon v + 2uv + \frac{N^2 - 9}{3N} v^2. \quad (37)$$

The exact normalization of the renormalized variables can be easily read from these series.

Since for $N = 2$ and 3 the two quartic terms are not independent, an appropriate combination of the above β functions must reproduce the β functions of the O(3) and O(8) Φ^4 theories. Indeed, using Eq. (17) and setting $g = u + v/2$, we obtain

$$\beta_u + \frac{1}{2}\beta_v = \beta_{\text{O}(3)}(g) = -\epsilon g + \frac{11}{6}g^2 \quad (38)$$

for $N = 2$, and

$$\beta_u + \frac{1}{2}\beta_v = \beta_{\text{O}(8)}(g) = -\epsilon g + \frac{8}{3}g^2 \quad (39)$$

for $N = 3$. These exact relations provide a stringent check of the five-loop series for the model (5), which must reproduce the corresponding series of the O(3) and O(8) vector models [28,29] for $N = 2$ and 3.

For $N \geq 4$ the FPs of the RG flow are given by the common zeros of the β functions (36) and (37). Their stability requires that the eigenvalues of the matrix $\Omega_{ij} = \partial\beta_{g_i}/\partial g_j$ (where $g_{1,2}$ correspond to u, v) have positive real part. In the standard ϵ -expansion scheme [30], the FPs, i.e., the common zeros of the β functions, are determined perturbatively as expansions in powers of $\epsilon \equiv 4 - d$, while exponents are obtained by expanding the corresponding RG functions computed at the FP in powers of ϵ .

A straightforward analysis of the one-loop β functions (36) and (37) finds four different FPs. Two of them have $v = 0$ and are always unstable. We have the trivial Gaussian FP at $(u = 0, v = 0)$, which is always unstable with respect to both quartic perturbations. There is also an O(M) symmetric FP with $M = N^2 - 1$ at

$$u = \epsilon \frac{6}{N^2 + 7}, \quad v = 0, \quad (40)$$

which can be shown, nonperturbatively, to be unstable with respect to the operator $\text{Tr } \Psi^4$. Indeed, such operator contains a spin-4 perturbation with respect to the O(M) group [16], which is relevant at the O(M)-symmetric FP for any $M > 4$ to O(ϵ), and for any $M \geq 3$ in three dimensions [7,31].

There are also two FPs with $v < 0$. One of them is stable, the other is unstable. However, they only exist for $N < N_{c,0}$,

with

$$N_{c,0} = \frac{3}{\sqrt{2}} \sqrt{1 + \sqrt{3}} \approx 3.506. \quad (41)$$

For $N = N_{c,0}$ these two FPs merge and then, for $N > N_{c,0}$, they become complex. For $N = 3$ the stable FP merges with the O(8) FP. These results show that, for integer values of N satisfying $N \geq 4$, there is no stable FP close to four dimensions, hence only first-order transitions are allowed.

2. Five-loop ϵ expansion analysis

In order to establish the behavior of the system for $\epsilon = 1$, we must determine the fate of the stable FP that exists for $N < N_{c,0}$ close to four dimensions. For finite ϵ , we expect a stable and an unstable FP with $v \neq 0$ up to $N = N_c(\epsilon)$. The two FPs merge for $N = N_c(\epsilon)$ and become complex for $N > N_c(\epsilon)$. In order to compute $N_c(\epsilon)$, we expand

$$N_c(\epsilon) = N_{c,0} + \sum_{n=1} N_{c,n} \epsilon^n, \quad (42)$$

and require

$$\beta_u(u, v, N_c) = \beta_v(u, v, N_c) = 0, \quad \det \Omega(u, v, N_c) = 0, \quad (43)$$

the last equation being a consequence of the coalescence of the two FPs at $N = N_c$. A straightforward calculation gives finally

$$N_c(\epsilon) = 3.5063 - 0.0309\epsilon + 0.3229\epsilon^2 - 1.2927\epsilon^3 \\ + 7.6855\epsilon^4 + O(\epsilon^5). \quad (44)$$

The expansion alternates in sign, as expected for a Borel-summable series. Resummations using the Padé-Borel method appear to be stable. We obtain $N_c(\epsilon = 1) = 3.54(1)$ using the series to order ϵ^3 and $N_c(\epsilon = 1) = 3.59(2)$ at order ϵ^4 (the number in parentheses indicates how the estimate changes by varying the resummation parameters). Apparently, N_c varies only slightly as ϵ changes from 0 to 1. In particular, this analysis predicts the absence of stable FPs for any integer $N \geq 4$ in three dimensions.

3. High-order analysis in three dimensions

Methods based on the expansion around four dimensions allow us to find only the 3D FPs which can be defined, by analytic continuation, close to four dimensions. Other FPs, which do not have a 4D counterpart, cannot be detected. However, the extension of this result to the relevant $d = 3$ dimension fails in some cases. For example, this also occurs for the Ginzburg-Landau model of superconductors, in which a complex scalar field couples to a gauge field: although ϵ -expansion calculations do not find a stable FP [32], thus predicting first-order transitions, numerical analyses of 3D systems described by the Ginzburg-Landau model show that they can also undergo continuous transitions (see, e.g., Refs. [33,34]). This implies the presence of a stable FP in the 3D Ginzburg-Landau theory, in agreement with experiments [35]. Other examples are provided by the LGW Φ^4 theories describing frustrated spin models with noncollinear order [36,37], the ^3He superfluid transition from the normal to the planar phase [38], and the chiral transitions of the

strong interactions in the case the $U(1)_A$ anomaly effects are suppressed [39,40].

Therefore, a more conclusive analysis requires a direct study of the 3D flow. This is achieved by an alternative analysis of the $\overline{\text{MS}}$ series: the 3D $\overline{\text{MS}}$ scheme without ϵ expansion [36,41,42]. The RG functions $\beta_{u,v}$ are the $\overline{\text{MS}}$ functions. However, $\epsilon \equiv 4 - d$ is no longer considered as a small quantity, but it is set equal to its physical value ($\epsilon = 1$ in our case) before looking for the FPs of the RG flow. This provides a well defined 3D perturbative scheme which allows us to compute universal quantities, without the need of expanding around $d = 4$ [41,42].

We look for stable FPs of the RG flow, with a finite attraction domain in the space of the renormalized couplings u and v . The RG trajectories are determined by solving the differential equations

$$-\lambda \frac{du}{d\lambda} = \beta_u(u(\lambda), v(\lambda)), \quad -\lambda \frac{dv}{d\lambda} = \beta_v(u(\lambda), v(\lambda)), \quad (45)$$

where $\lambda \in [0, \infty)$, with the initial conditions

$$u(0) = v(0) = 0, \quad \left. \frac{du}{d\lambda} \right|_{\lambda=0} = s \equiv \frac{u_0}{|v_0|}, \quad \left. \frac{dv}{d\lambda} \right|_{\lambda=0} = \pm 1, \quad (46)$$

where s parametrizes the different RG trajectories in terms of the bare quartic parameters, and the \pm sign corresponds to the RG flows for positive and negative values of v_0 . In our study of the RG flow we only consider values of the bare couplings which satisfy Eqs. (7) and (8).

The physically relevant results are obtained by resumming the perturbative expansions, which are divergent but Borel summable in a large region of the renormalized parameters. The resummation can be done exploiting methods that take into account their large-order behavior, which is computed by semiclassical (hence, intrinsically nonperturbative) instanton calculations [24,27,31]. Relevant results for the large-order behavior of the series of the model (5) are reported in Appendix C.

B. 3D MZM perturbative scheme

In the massive zero-momentum (MZM) scheme [5,27,43,44] one performs the perturbative expansion directly in three dimensions, in the critical region of the disordered phase, in powers of the zero-momentum renormalized quartic couplings. The theory is renormalized by introducing a set of zero-momentum conditions for the one-particle irreducible two-point and four-point correlation functions of the 2×2 matrix field Ψ :

$$\Gamma_{a_1 a_2, b_1 b_2}^{(2)}(p) = \left(\delta_{a_1 b_2} \delta_{a_2 b_1} - \frac{1}{N} \delta_{a_1 a_2} \delta_{b_1 b_2} \right) \times Z_\psi^{-1} [m^2 + p^2 + O(p^4)], \quad (47)$$

$$\Gamma_{a_1 a_2, b_1 b_2, c_1 c_2, d_1 d_2}^{(4)}(0) = Z_\psi^{-2} m^{4-d} (u U_{a_1 a_2, b_1 b_2, c_1 c_2, d_1 d_2} + v V_{a_1 a_2, b_1 b_2, c_1 c_2, d_1 d_2}), \quad (48)$$

where U, V are appropriate form factors defined so that $u \propto u_0/m$ and $v \propto v_0/m$ at the leading tree order. The FPs of the theory are given by the common zeros of the Callan-Symanzik β functions

$$\beta_u(u, v) = m \left. \frac{\partial u}{\partial m} \right|_{u_0, v_0}, \quad \beta_v(u, v) = m \left. \frac{\partial v}{\partial m} \right|_{u_0, v_0}. \quad (49)$$

The normalization of the zero-momentum quartic variables u, v is such that their one-loop β functions read as

$$\beta_u = -u + u^2 + \frac{4N^4 + 22N^2 - 42}{N(N^2 + 7)^2} uv + \frac{3N^4 + 30N^2 + 63}{N^2(N^2 + 7)^2} v^2, \quad (50)$$

$$\beta_v = -v + \frac{12}{N^2 + 7} uv + \frac{2N^4 - 4N^2 - 126}{N(N^2 + 7)^2} v^2. \quad (51)$$

We compute the MZM perturbative expansions of the β functions and of the critical exponents up to six loops, requiring the computation of 1428 Feynman diagrams. The complete expansion for $N = 4$ can be found in Appendix B. The large-order behaviors of the series are reported in Appendix C. The RG trajectories are obtained by solving differential equations analogous to Eqs. (45) and (46), after resumming the β functions as outlined in Appendix C.

C. Results

Some RG trajectories in the renormalized coupling space of the LGW theory (5) for $N = 4$ are shown in Figs. 5 and 6, for the $\overline{\text{MS}}$ and MZM schemes, respectively, for several values of the ratio $s \equiv u_0/|v_0|$. In both renormalization schemes, most of the RG trajectories flow towards the region in which the

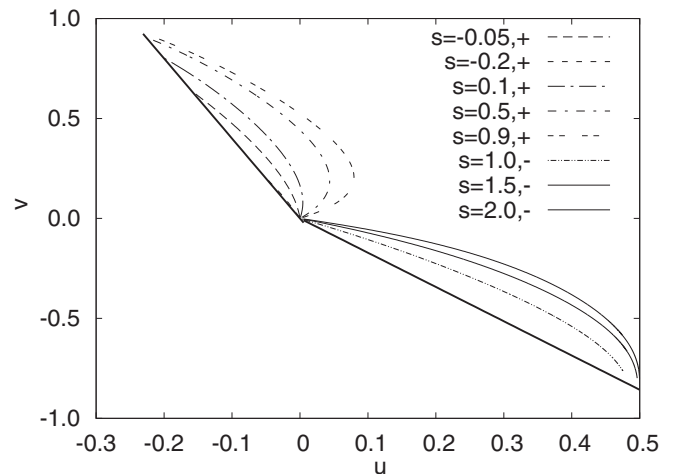


FIG. 5. RG flow of the LGW theory (5) for $N = 4$, in the $\overline{\text{MS}}$ scheme without ϵ expansion, for several values of the ratio $s \equiv u_0/|v_0|$ of the bare quartic parameters. The curves are obtained by solving Eqs. (45) with the initial conditions (46): in the legend we report the value of s and the sign of v_0 (“+” and “-” correspond to $v_0 > 0$ and $v_0 < 0$, respectively). The two solid lines represent the boundary of the Borel-summability region, defined by $u + v/4 > 0$ and $u + 7v/12 > 0$.

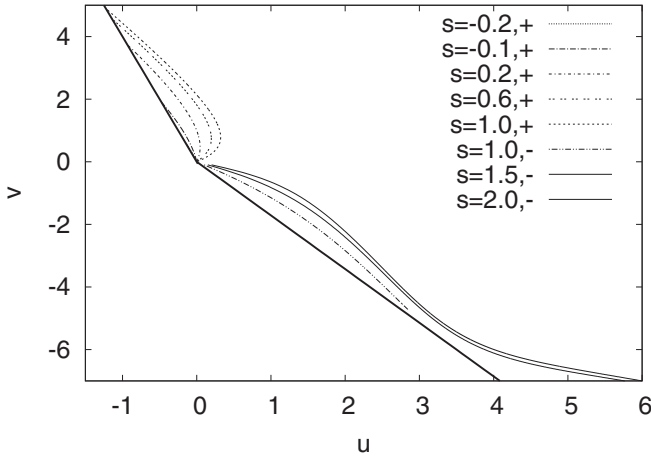


FIG. 6. RG flow of the LGW theory (5) for $N = 4$, in the MZM scheme, for several values of the ratio $s \equiv u_0/|v_0|$ of the bare quartic parameters. The curves are obtained by solving Eqs. (45) with the initial conditions (46): in the legend we report the value of s and the sign of v_0 (“+” and “-” correspond to $v_0 > 0$ and $v_0 < 0$, respectively). The two solid lines represent the boundary of the Borel-summability region, defined by $u + v/4 > 0$ and $u + 7v/12 > 0$.

series are no longer Borel summable. In the MZM scheme, for $v_0 < 0$ some trajectories flow instead towards infinity. In all cases, we do not have evidence of a stable FP. Analogous results are obtained for $N = 6$.

These results imply that there is no universality class characterized by the symmetry breakings (11) and (13). This would suggest a first-order transition. It is also possible that more than one transition is present, each of them associated to a partial decoupling of some degrees of freedom, hence to a different symmetry-breaking pattern, as it happens in two-dimensional frustrated XY models [45]. In this case, continuous transition would still be possible.

V. CONCLUSIONS

We have investigated the nature of the phase transitions in 3D ACP^{N-1} models, such as the lattice model (1) with $J > 0$, which are characterized by a global $U(N)$ symmetry and a local $U(1)$ gauge symmetry.

In order to analyze their critical behavior, we construct the corresponding LGW theory, assuming a staggered local gauge-invariant order parameter. This leads to the LGW Ψ^4 theory (5), where Ψ is a traceless Hermitian $N \times N$ matrix, which is symmetric under the global $U(N)$ transformations $\Psi \rightarrow U\Psi U^\dagger$, and the \mathbb{Z}_2 transformations $\Psi \rightarrow -\Psi$. For $N = 3$, the LGW model is equivalent to the one associated with an eight-component real vector field. Hence, we predict that, if the ACP^2 model undergoes a continuous transition, it should belong to the $O(8)$ vector universality class. Note that, at the critical point, there is an effective symmetry enlargement $U(3) \rightarrow O(8)$, and the same should occur in the low-temperature phase as the critical point is approached. The low-temperature symmetry $U(1) \times U(2)$ should be promoted to $O(7)$. We confirm the RG predictions by comparing the FSS behavior of the $O(8)$ vector and ACP^2 models,

obtained by MC simulations of both lattice models. We note that the critical behavior, characterized by the $O(8)$ critical exponents $\nu = 0.85(2)$ and $\eta = 0.0276(5)$, definitely differs from that of ferromagnetic CP^2 models, for which recent studies [2,8,10,11] have provided numerical evidence of continuous transitions with critical exponents $\nu = 0.536(13)$ and $\eta = 0.23(2)$.

In the case of ACP^{N-1} lattice models with a higher number of components, i.e., $N \geq 4$, the identification of the order parameter is more complex. If the order parameter is a staggered local gauge-invariant Hermitian matrix as for $N = 2$ and 3, the associated LGW theory is that given in Eq. (5). To determine the possible existence of continuous transitions, we study the RG flow in perturbation theory. We compute FT perturbative series in two different renormalization schemes up to five and six loops, respectively. The analysis of the RG flow does not provide evidence of stable FPs. This implies that the dynamics of the staggered gauge-invariant modes associated with the $N \times N$ Hermitian matrices defined in Eq. (4) does not give rise to continuous transitions. In particular, we do not expect continuous transitions characterized by the symmetry breaking $U(N) \rightarrow U(1) \times U(N-1)$. Thus, if the ACP^{N-1} lattice model presents transitions with this symmetry breaking, they must be first order. Note that it is still possible to have continuous transitions if they are associated with a different symmetry breaking, as it may arise from a partial decoupling of some degrees of freedom. Another possible scenario may arise from the relevance of further gauge degrees of freedom which are not taken into account by the LGW theory, analogously to the case of ferromagnetic CP^{N-1} model in the large- N limit. This issue needs further investigation.

APPENDIX A: GROUND STATE FOR THE ANTIFERROMAGNETIC MODEL WITH $N = 3$

In this section, we wish to characterize the structure of the ground state of the antiferromagnetic model for $N = 3$, showing the emergence of a ferromagnetic order on a staggered lattice. Let us first consider a lattice plaquette [see Fig. 7(a)], and let us determine the configurations of the four spins z_1, z_2, z_3 , and z_4 that minimize the energy. Given the global invariance of the model, it is not restrictive to assume that $z_1 = (1, 0, 0)$. Since the model is antiferromagnetic, the energy is minimized if neighboring spins are orthogonal, i.e., if $\bar{z}_i \cdot z_j = 0$ for nearest neighbor sites i and j . Therefore, we have

$$z_2 = (0, v_2), \quad z_4 = (0, v_4), \quad (\text{A1})$$

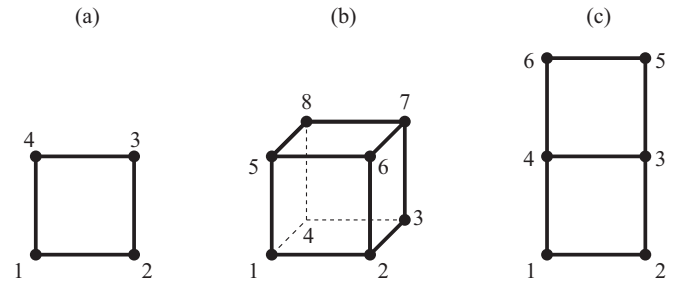


FIG. 7. We draw some lattice configurations required by the discussion of Appendix A.

where \mathbf{v}_2 and \mathbf{v}_4 are two-dimensional complex unit vectors. If we set $\mathbf{z}_3 = (z_{31}, \mathbf{v}_3)$ and consider the links connecting site 3 with its neighbors, we obtain the conditions

$$\bar{\mathbf{v}}_2 \cdot \mathbf{v}_3 = \bar{\mathbf{v}}_4 \cdot \mathbf{v}_3 = 0. \quad (\text{A2})$$

If $\mathbf{v}_2 \neq e^{i\phi} \mathbf{v}_4$ (ϕ is an arbitrary phase), this condition implies $\mathbf{v}_3 = 0$. Therefore, discarding an irrelevant phase, we obtain $\mathbf{z}_1 = \mathbf{z}_3$. Instead if $\mathbf{v}_2 = e^{i\phi} \mathbf{v}_4$, eliminating an irrelevant phase we obtain $\mathbf{z}_2 = \mathbf{z}_4$. This analysis shows, therefore, that in the ground-state configuration two opposite spins in the plaquette are identical. Note that the result holds only for $N = 3$. For $N \geq 4$, Eq. (A2) does not imply $\mathbf{v}_3 = 0$ in the generic case. We only obtain that \mathbf{z}_3 belongs to $(N - 2)$ -dimensional subspace containing \mathbf{z}_1 . This may leave open the possibility of other symmetry-breaking patterns for $N > 3$.

Let us now assume that we are dealing with a three-dimensional system and let us consider a cube [see Fig. 7(b)]. We wish now to show that the dominant ground-state configurations have the following structure. One can have $\mathbf{z}_1 = \mathbf{z}_3 = \mathbf{z}_6 = \mathbf{z}_8$ (we properly fix the phases), while $\mathbf{z}_2, \mathbf{z}_4, \mathbf{z}_5, \mathbf{z}_7$ are arbitrary spins lying in the complex two-dimensional plane orthogonal to \mathbf{z}_1 . Of course, the equivalent arrangement with $\mathbf{z}_2 = \mathbf{z}_4 = \mathbf{z}_5 = \mathbf{z}_7$ is also possible. Note that this configuration is highly degenerate, as four two-dimensional vectors can be arbitrarily chosen.

To prove the previous statement, we consider all other possible arrangements that are consistent with the result obtained for the plaquette and we show that they are less degenerate than the one discussed before. Hence, they are entropically disfavored and become irrelevant in the infinite-volume limit. It is not restrictive to assume that $\mathbf{z}_1 = \mathbf{z}_3 = (1, 0, 0)$ since two opposite spins of plaquette $\langle 1, 2, 3, 4 \rangle$ (we report in angular brackets the sites belonging to the plaquette) are necessarily identical. Let us now consider the plaquette $\langle 5, 6, 7, 8 \rangle$. There are three different possibilities consistent with the result valid for a single plaquette: (i) $\mathbf{z}_6 = \mathbf{z}_8$ and $\mathbf{z}_6 = \mathbf{z}_1$; (ii) $\mathbf{z}_6 = \mathbf{z}_8$ with $\mathbf{z}_6 \neq e^{i\phi} \mathbf{z}_1$; (iii) $\mathbf{z}_5 = \mathbf{z}_7$. We wish now to exclude cases (ii) and (iii). In case (ii), the orthogonality condition applied

to links (1,2) and (2,6) implies

$$\bar{\mathbf{z}}_1 \cdot \mathbf{z}_2 = \bar{\mathbf{z}}_6 \cdot \mathbf{z}_2 = 0. \quad (\text{A3})$$

Since $\mathbf{z}_6 \neq e^{i\phi} \mathbf{z}_1$, these two conditions completely specify vector \mathbf{z}_2 (the phase is of course irrelevant). Repeating the argument to the spins at sites 2,4,5,7 we end up with

$$\mathbf{z}_2 = \mathbf{z}_4 = \mathbf{z}_5 = \mathbf{z}_7. \quad (\text{A4})$$

It is therefore a configuration of type (i), but now the spins are ordered on the complementary sites 2,4,5,7. Let us now consider case (iii). Generically, $\mathbf{z}_2 \neq e^{i\phi} \mathbf{z}_5$ and $\mathbf{z}_4 \neq e^{i\phi} \mathbf{z}_5$. This implies that \mathbf{z}_6 and \mathbf{z}_8 are uniquely defined. Therefore, the configuration is defined by specifying $\mathbf{z}_2, \mathbf{z}_4$, and \mathbf{z}_5 in the two-dimensional complex space orthogonal to \mathbf{z}_1 . This configuration is less degenerate than that defined at point (i), hence it is irrelevant in the infinite-volume limit (it is entropically suppressed). If $\mathbf{z}_2 = e^{i\phi} \mathbf{z}_5$ and $\mathbf{z}_4 \neq e^{i\phi} \mathbf{z}_5$, we obtain the same type of degeneracy since now $\mathbf{z}_4, \mathbf{z}_5$, and \mathbf{z}_6 can be chosen. The other two cases give the same result.

The result for a cube extends trivially to the whole lattice, proving that in the ground state we observe two different symmetry breakings. First, lattice translational invariance is broken with the emergence of a staggered symmetry. Second, on one of the two sublattices the system orders ferromagnetically, breaking the $U(3)$ symmetry down to $U(2)$. It is important to note that the discussion only applies in three dimensions. In two dimensions, the results do not hold. Indeed, referring to Fig. 7(c), nothing forbids in the two-dimensional case a configuration with $\mathbf{z}_1 = \mathbf{z}_3, \mathbf{z}_4 = \mathbf{z}_5$, and $\mathbf{z}_6 \neq \mathbf{z}_3$.

APPENDIX B: HIGH-ORDER FIELD-THEORETICAL PERTURBATIVE EXPANSIONS

In this appendix, we report the FT perturbative series of the β functions used in our RG analysis of Sec. IV. We only report those for $N = 4$; the perturbative series for other values of N are available on request.

The five-loop β functions of the $\overline{\text{MS}}$ scheme for $N = 4$ are

$$\begin{aligned} \beta_u(u, v) = & -\varepsilon u + \frac{23}{6} u^2 - \frac{59}{12} u^3 + \frac{24215}{1728} u^4 - \frac{2808613}{62208} u^5 + \frac{2231}{19440} \pi^4 u^5 + \frac{37543651}{221184} u^6 - \frac{45935}{41472} \pi^4 u^6 - \frac{56005}{326592} \pi^6 u^6 \\ & + \frac{29}{12} uv - \frac{319}{72} u^2 v + \frac{72587}{3456} u^3 v - \frac{2556031}{31104} u^4 v + \frac{2639}{15552} \pi^4 u^4 v + \frac{4691425207}{11943936} u^5 v - \frac{4445671}{1866240} \pi^4 u^5 v \\ & - \frac{689765}{1959552} \pi^6 u^5 v + \frac{19}{32} v^2 - \frac{1129}{576} uv^2 + \frac{210121}{13824} u^2 v^2 - \frac{36468307}{497664} u^3 v^2 + \frac{17129}{155520} \pi^4 u^3 v^2 + \frac{42566947705}{95551488} u^4 v^2 \\ & - \frac{71427821}{29859840} \pi^4 u^4 v^2 - \frac{5358835}{15676416} \pi^6 u^4 v^2 - \frac{83}{192} v^3 + \frac{10789}{2048} uv^3 - \frac{35875069}{995328} u^2 v^3 + \frac{27641}{622080} \pi^4 u^2 v^3 \\ & + \frac{27514775011}{95551488} u^3 v^3 - \frac{21388189}{14929920} \pi^4 u^3 v^3 - \frac{9436835}{47029248} \pi^6 u^3 v^3 + \frac{243899}{442368} v^4 - \frac{139893917}{15925248} uv^4 + \frac{64219}{4976640} \pi^4 uv^4 \\ & + \frac{158989734779}{1528823808} u^2 v^4 - \frac{17049203}{31850496} \pi^4 u^2 v^4 - \frac{55096345}{752467968} \pi^6 u^2 v^4 - \frac{13810271}{15925248} v^5 + \frac{38971}{19906560} \pi^4 v^5 \\ & + \frac{60552906587}{3057647616} uv^5 - \frac{6124463}{53084160} \pi^4 uv^5 - \frac{3213535}{214990848} \pi^6 uv^5 + \frac{39907063243}{24461180928} v^6 - \frac{83027651}{7644119040} \pi^4 v^6 \\ & - \frac{4971655}{4013162496} \pi^6 v^6 + \frac{97}{18} u^4 \zeta(3) - \frac{27967}{648} u^5 \zeta(3) + \frac{1058293}{4608} u^6 \zeta(3) + \frac{58}{9} u^3 v \zeta(3) - \frac{400519}{5184} u^4 v \zeta(3) \\ & + \frac{127075013}{248832} u^5 v \zeta(3) + \frac{203}{48} u^2 v^2 \zeta(3) - \frac{232333}{3456} u^3 v^2 \zeta(3) + \frac{371192045}{663552} u^4 v^2 \zeta(3) + \frac{83}{48} uv^3 \zeta(3) \\ & - \frac{697141}{20736} u^2 v^3 \zeta(3) + \frac{242855651}{663552} u^3 v^3 \zeta(3) + \frac{1271}{4608} v^4 \zeta(3) - \frac{742109}{82944} uv^4 \zeta(3) + \frac{4536772733}{31850496} u^2 v^4 \zeta(3) \\ & - \frac{1246357}{1327104} v^5 \zeta(3) + \frac{211486009}{7077888} uv^5 \zeta(3) + \frac{435745159}{169869312} v^6 \zeta(3) - \frac{291}{32} u^6 \zeta(3)^2 - \frac{113129}{5184} u^5 v \zeta(3)^2 \\ & - \frac{887615}{41472} u^4 v^2 \zeta(3)^2 - \frac{1485335}{124416} u^3 v^3 \zeta(3)^2 - \frac{8714053}{1990656} u^2 v^4 \zeta(3)^2 - \frac{4430365}{3981312} uv^5 \zeta(3)^2 - \frac{1655603}{10616832} v^6 \zeta(3)^2 \end{aligned}$$

$$\begin{aligned}
& -\frac{2435}{54}u^5\zeta(5) + \frac{431011}{864}u^6\zeta(5) - \frac{2755}{36}u^4v\zeta(5) + \frac{2847481}{2592}u^5v\zeta(5) - \frac{85975}{1296}u^3v^2\zeta(5) + \frac{15884369}{13824}u^4v^2\zeta(5) \\
& -\frac{43825}{1296}u^2v^3\zeta(5) + \frac{5504765}{7776}u^3v^3\zeta(5) - \frac{364135}{41472}uv^4\zeta(5) + \frac{518304421}{1990656}u^2v^4\zeta(5) - \frac{11345}{13824}v^5\zeta(5) \\
& + \frac{104582551}{1990656}uv^5\zeta(5) + \frac{15744751}{3538944}v^6\zeta(5) + \frac{319039}{864}u^6\zeta(7) + \frac{444773}{576}u^5v\zeta(7) + \frac{3807055}{4608}u^4v^2\zeta(7) + \frac{7509005}{13824}u^3v^3\zeta(7) \\
& + \frac{15674365}{73728}u^2v^4\zeta(7) + \frac{733383}{16384}uv^5\zeta(7) + \frac{1518167}{393216}v^6\zeta(7), \tag{B1}
\end{aligned}$$

$$\begin{aligned}
\beta_v(u, v) = & -\varepsilon v + 2uv - \frac{157}{36}u^2v + \frac{5879}{864}u^3v - \frac{685387}{20736}u^4v + \frac{19}{108}\pi^4u^4v + \frac{4545155}{46656}u^5v - \frac{989059}{933120}\pi^4u^5v - \frac{24925}{122472}\pi^6u^5v \\
& + \frac{7}{12}v^2 - \frac{229}{72}uv^2 + \frac{5921}{864}u^2v^2 - \frac{3207107}{62208}u^3v^2 + \frac{1073}{3888}\pi^4u^3v^2 + \frac{2236916635}{11943936}u^4v^2 - \frac{379369}{186624}\pi^4u^4v^2 \\
& - \frac{767575}{1959552}\pi^6u^4v^2 - \frac{29}{64}v^3 + \frac{40699}{13824}uv^3 - \frac{5568277}{165888}u^2v^3 + \frac{12247}{77760}\pi^4u^2v^3 + \frac{2050563751}{11943936}u^3v^3 \\
& - \frac{11735557}{7464960}\pi^4u^3v^3 - \frac{1806125}{5878656}\pi^6u^3v^3 + \frac{5885}{9216}v^4 - \frac{3433885}{331776}uv^4 + \frac{133}{3456}\pi^4uv^4 + \frac{8406050713}{95551488}u^2v^4 \\
& - \frac{381881}{622080}\pi^4u^2v^4 - \frac{11779825}{94058496}\pi^6u^2v^4 - \frac{18033929}{15925248}v^5 + \frac{4}{1215}\pi^4v^5 + \frac{4316967439}{191102976}uv^5 - \frac{9687473}{79626240}\pi^4uv^5 \\
& - \frac{5139325}{188116992}\pi^6uv^5 + \frac{6609591883}{3057647616}v^6 - \frac{2367521}{238878720}\pi^4v^6 - \frac{163685}{62705664}\pi^6v^6 + \frac{58}{9}u^3v\zeta(3) - \frac{4987}{144}u^4v\zeta(3) \\
& + \frac{2807371}{15552}u^5v\zeta(3) + \frac{43}{6}u^2v^2\zeta(3) - \frac{132667}{2592}u^3v^2\zeta(3) + \frac{3169315}{9216}u^4v^2\zeta(3) + \frac{175}{72}uv^3\zeta(3) - \frac{75677}{2592}u^2v^3\zeta(3) \\
& + \frac{2558749}{9216}u^3v^3\zeta(3) + \frac{145}{576}v^4\zeta(3) - \frac{326005}{41472}uv^4\zeta(3) + \frac{235439287}{1990656}u^2v^4\zeta(3) - \frac{300469}{331776}v^5\zeta(3) \\
& + \frac{8893439}{331776}uv^5\zeta(3) + \frac{6145307}{2359296}v^6\zeta(3) - \frac{1099}{324}u^5v\zeta(3)^2 - \frac{33215}{5184}u^4v^2\zeta(3)^2 - \frac{37625}{15552}u^3v^3\zeta(3)^2 \\
& + \frac{364091}{248832}u^2v^4\zeta(3)^2 + \frac{650747}{497664}uv^5\zeta(3)^2 + \frac{88027}{331776}v^6\zeta(3)^2 - \frac{2485}{54}u^4v\zeta(5) + \frac{540673}{1296}u^5v\zeta(5) - \frac{11035}{162}u^3v^2\zeta(5) \\
& + \frac{228535}{288}u^4v^2\zeta(5) - \frac{50945}{1296}u^2v^3\zeta(5) + \frac{19449871}{31104}u^3v^3\zeta(5) - \frac{59095}{5184}uv^4\zeta(5) + \frac{4044073}{15552}u^2v^4\zeta(5) \\
& - \frac{7285}{4608}v^5\zeta(5) + \frac{58034203}{995328}uv^5\zeta(5) + \frac{3784553}{663552}v^6\zeta(5) + \frac{29155}{72}u^5v\zeta(7) + \frac{221725}{288}u^4v^2\zeta(7) + \frac{354515}{576}u^3v^3\zeta(7) \\
& + \frac{2424275}{9216}u^2v^4\zeta(7) + \frac{560413}{9216}uv^5\zeta(7) + \frac{683795}{110592}v^6\zeta(7). \tag{B2}
\end{aligned}$$

The six-loop β functions of the MZM scheme for $N = 4$ are

$$\begin{aligned}
\beta_u(u, v) = & -u + u^2 - 0.22544283u^3 + 0.10908673u^4 - 0.06576687u^5 + 0.04692261u^6 - 0.03823225u^7 \\
& + 0.63043478uv - 0.20303858u^2v + 0.15749967u^3v - 0.11634780u^4v + 0.10631128u^5v - 0.10058595u^6v \\
& + 0.15489130v^2 - 0.08970454uv^2 + 0.11442230u^2v^2 - 0.10401712u^3v^2 + 0.12188821u^4v^2 - 0.13382427u^5v^2 \\
& - 0.01961248v^3 + 0.04186104uv^3 - 0.05255068u^2v^3 + 0.08208912u^3v^3 - 0.10859850u^4v^3 + 0.00498971v^4 \\
& - 0.01301539uv^4 + 0.03157946u^2v^4 - 0.05477669u^3v^4 - 0.00117098v^5 + 0.00642308uv^5 - 0.01679641u^2v^5 \\
& + 0.00054799v^6 - 0.00289150uv^6 - 0.00021554v^7, \tag{B3}
\end{aligned}$$

$$\begin{aligned}
\beta_v(u, v) = & -v + 0.52173913uv - 0.20023805u^2v + 0.06703734u^3v - 0.05601881u^4v + 0.03225406u^5v \\
& - 0.03176901u^6v + 0.15217391v^2 - 0.14632780uv^2 + 0.06972703u^2v^2 - 0.08566328u^3v^2 + 0.06017577u^4v^2 \\
& - 0.07408173u^5v^2 - 0.02133655v^3 + 0.02700191uv^3 - 0.05410921u^2v^3 + 0.05068529u^3v^3 - 0.07920335u^4v^3 \\
& + 0.00462087v^4 - 0.01692328uv^4 + 0.02380079u^2v^4 - 0.04877347u^3v^4 - 0.00215837v^5 + 0.00591753uv^5 \\
& - 0.01769814u^2v^5 + 0.00059843v^6 - 0.00351442uv^6 - 0.00029807v^7. \tag{B4}
\end{aligned}$$

APPENDIX C: SUMMATION OF THE PERTURBATIVE SERIES

Since perturbative expansions are divergent, resummation methods must be used to obtain meaningful results. Given a generic quantity $S(u, v)$ with perturbative expansion $S(u, v) = \sum_{ij} c_{ij}u^i v^j$, we consider

$$S(xu, xv) = \sum_k s_k(u, v)x^k, \tag{C1}$$

which must be evaluated at $x = 1$. The expansion (C1) in powers of x is resummed by using the conformal-mapping

method [27] that exploits the knowledge of the large-order behavior of the coefficients, generally given by

$$s_k(u, v) \sim k! [-A(u, v)]^k k^b [1 + O(k^{-1})]. \tag{C2}$$

The quantity $A(u, v)$ is related to the singularity t_s of the Borel transform $B(t)$ that is nearest to the origin: $t_s = -1/A(u, v)$. The series is Borel summable for $x > 0$ if $B(t)$ does not have singularities on the positive real axis, and, in particular, if $A(u, v) > 0$. The large-order behavior can be determined using semiclassical computations, based on the computations of appropriate instanton configurations [24,27]. For even N , these semiclassical calculations show that the expansion is

Borel summable when

$$u + b_N v > 0, \quad u + \frac{1}{N} v > 0, \quad (\text{C3})$$

where b_N is given in Eq. (7). For odd N we obtain analogously

$$u + b_N v > 0, \quad u + c_N v > 0, \quad (\text{C4})$$

where c_N is given in Eq. (9). Note that the conditions for Borel summability on the renormalized couplings correspond to the stability conditions (7) and (8) of the bare quartic couplings. In this Borel-summability region we have for even N

$$A(u, v) = \frac{1}{2} \text{Max}(u + b_N v, u + v/N). \quad (\text{C5})$$

For odd N , we should replace $u + v/N$ with $u + c_N v$. Under the additional assumption that the Borel-transform

singularities lie only in the negative axis, the conformal-mapping method turns the original expansion into a convergent one in the region (C3). Outside, the expansion is not Borel summable.

Analogously, one can derive the large-order behavior of the MZM scheme, which is again given by Eq. (C2) but with

$$A(u, v) = \frac{1.32997}{N^2 + 7} \text{Max}(u + b_N v, u + v/N) \quad (\text{C6})$$

for even N . For odd values of N , $u + v/N$ should be replaced with $u + c_N v$.

We use the conformal mapping method to resum the series taking into account what we know about their large-order behavior. The method we use is described in Refs. [27,31]. Resummations depend on two parameters, which are optimized in the procedure. Using the notations of Refs. [27,31], the approximants we use depend on two parameters α and b .

-
- [1] N. Read and S. Sachdev, *Phys. Rev. B* **42**, 4568 (1990).
 - [2] R. K. Kaul, *Phys. Rev. B* **85**, 180411(R) (2012).
 - [3] R. K. Kaul and A. W. Sandvik, *Phys. Rev. Lett.* **108**, 137201 (2012).
 - [4] M. S. Block, R. G. Melko, and R. K. Kaul, *Phys. Rev. Lett.* **111**, 137202 (2013).
 - [5] A. Pelissetto and E. Vicari, *Phys. Rep.* **368**, 549 (2002).
 - [6] M. Campostrini, M. Hasenbusch, A. Pelissetto, P. Rossi, and E. Vicari, *Phys. Rev. B* **65**, 144520 (2002).
 - [7] M. Hasenbusch and E. Vicari, *Phys. Rev. B* **84**, 125136 (2011).
 - [8] A. Nahum, J. T. Chalker, P. Serna, M. Ortuno, and A. M. Somoza, *Phys. Rev. B* **88**, 134411 (2013).
 - [9] We remind the reader of these simple relations valid for any generic 2×2 matrix: $\text{Tr} A^3 = \frac{3}{2}(\text{Tr} A^2)(\text{Tr} A) - \frac{1}{2}(\text{Tr} A)^3$; $\text{Tr} A^4 = -\frac{1}{2}(\text{Tr} A)^4 + (\text{Tr} A)^2 \text{Tr} A^2 + \frac{1}{2}(\text{Tr} A^2)^2$. If additionally $\text{Tr} A = 0$, we obtain $\text{Tr} A^3 = 0$ and $\text{Tr} A^4 = \frac{1}{2}(\text{Tr} A^2)^2$.
 - [10] A. Nahum, J. T. Chalker, P. Serna, M. Ortuno, and A. M. Somoza, *Phys. Rev. Lett.* **107**, 110601 (2011).
 - [11] K. Kataoka, S. Hattori, and I. Ichinose, *Phys. Rev. B* **83**, 174449 (2011).
 - [12] M. Moshe and J. Zinn-Justin, *Phys. Rep.* **385**, 69 (2003).
 - [13] L. A. Fernandez, V. Martín-Mayor, D. Sciretti, A. Tarancón, and J. L. Velasco, *Phys. Lett. B* **628**, 281 (2005).
 - [14] J. L. Alonso, A. Cruz, L. A. Fernandez, S. Jimenez, V. Martín-Mayor, J. J. Ruiz-Lorenzo, and A. Tarancón, *Phys. Rev. B* **71**, 014420 (2005).
 - [15] F. Basile, A. Pelissetto, and E. Vicari, *J. High Energy Phys.* **02** (2005) 044.
 - [16] P. Calabrese, A. Pelissetto, and E. Vicari, *Phys. Rev. B* **67**, 054505 (2003).
 - [17] M. De Prato, A. Pelissetto, and E. Vicari, *Phys. Rev. B* **68**, 092403 (2003).
 - [18] B. Nienhuis and M. Nauenberg, *Phys. Rev. Lett.* **35**, 477 (1975).
 - [19] M. E. Fisher and A. N. Berker, *Phys. Rev. B* **26**, 2507 (1982).
 - [20] V. Privman and M. E. Fisher, *J. Stat. Phys.* **33**, 385 (1983).
 - [21] S. A. Antonenko and A. I. Sokolov, *Phys. Rev. E* **51**, 1894 (1995).
 - [22] P. Butera and M. Comi, *Phys. Rev. B* **56**, 8212 (1997).
 - [23] G. A. Baker, Jr., B. G. Nickel, M. S. Green, and D. I. Meiron, *Phys. Rev. Lett.* **36**, 1351 (1976); G. A. Baker, Jr., B. G. Nickel, and D. I. Meiron, *Phys. Rev. B* **17**, 1365 (1978).
 - [24] J. C. Le Guillou and J. Zinn-Justin, *Phys. Rev. Lett.* **39**, 95 (1977); *Phys. Rev. B* **21**, 3976 (1980).
 - [25] R. Guida and J. Zinn-Justin, *J. Phys. A: Math. Gen.* **31**, 8103 (1998).
 - [26] G. 't Hooft and M. J. G. Veltman, *Nucl. Phys. B* **44**, 189 (1972).
 - [27] J. Zinn-Justin, *Quantum Field Theory and Critical Phenomena*, 4th ed. (Clarendon, Oxford, 2002).
 - [28] K. G. Chetyrkin, S. G. Gorishny, S. A. Larin, and F. V. Tkachov, *Phys. Lett. B* **132**, 351 (1983).
 - [29] H. Kleinert, J. Neu, V. Schulte-Frohlinde, K. G. Chetyrkin, and S. A. Larin, *Phys. Lett. B* **272**, 39 (1991); **319**, 545 (1993) (erratum).
 - [30] K. G. Wilson and M. E. Fisher, *Phys. Rev. Lett.* **28**, 240 (1972).
 - [31] J. M. Carmona, A. Pelissetto, and E. Vicari, *Phys. Rev. B* **61**, 15136 (2000).
 - [32] B. I. Halperin, T. C. Lubensky, and S. K. Ma, *Phys. Rev. Lett.* **32**, 292 (1974).
 - [33] S. Mo, J. Hove, and A. Sudbø, *Phys. Rev. B* **65**, 104501 (2002).
 - [34] F. S. Nogueira and H. Kleinert, in *Order, Disorder, and Criticality*, edited by Y. Holovatch (World Scientific, Singapore, 2007).
 - [35] C. W. Garland and G. Nounesis, *Phys. Rev. E* **49**, 2964 (1994).
 - [36] P. Calabrese, P. Parruccini, A. Pelissetto, and E. Vicari, *Phys. Rev. B* **70**, 174439 (2004).
 - [37] Y. Nakayama and T. Ohtsuki, *Phys. Rev. D* **91**, 021901 (2015).
 - [38] M. De Prato, A. Pelissetto, and E. Vicari, *Phys. Rev. B* **70**, 214519 (2004).
 - [39] A. Pelissetto and E. Vicari, *Phys. Rev. D* **88**, 105018 (2013).
 - [40] R. D. Pisarski and F. Wilczek, *Phys. Rev. D* **29**, 338 (1984).
 - [41] V. Dohm, *Z. Phys. B* **60**, 61 (1985); **61**, 193 (1985).
 - [42] R. Schloms and V. Dohm, *Nucl. Phys. B* **328**, 639 (1989).
 - [43] E. Vicari, [arXiv:0709.1014](https://arxiv.org/abs/0709.1014).
 - [44] G. Parisi, Cargèse Lectures (1973) (unpublished); *J. Stat. Phys.* **23**, 49 (1980).
 - [45] M. Hasenbusch, A. Pelissetto, and E. Vicari, *J. Stat. Mech.* (2005) P12002; *Phys. Rev. B* **72**, 184502 (2005).